

Supporting Information

Valence states of single Au atoms dictate catalytic activity of $\text{Au}_1/\text{CeO}_2(100)$

Rui Liu,^a Weiye Qu,^a Xiaolei Hu,^a Junxiao Chen,^a Yangyang Dong,^a Dongrun Xu,^a
Jing Liu,^a Zhen Ma,^{*ac} Xingfu Tang ^{*abc}

^a *Department of Environmental Science & Engineering, Fudan University, 2005 Songhu Road, Shanghai 200438, China.*

^b *Jiangsu Collaborative Innovation Center of Atmospheric Environment & Equipment Technology, Nanjing University of Information Science & Technology, Nanjing 210044, China.*

^c *Shanghai Institute of Pollution Control and Ecological Security, Shanghai 200092, China.*

Contents

1. Experimental Section	3
1.1. Catalyst Preparation.....	3
1.2. Catalyst Characterization.....	3
1.3. Catalytic Evaluation.	5
2. Figures and Table	6
Table S1. The XPS result detail of Au 4 <i>f</i> of Au- δ	6
Table S2. The XPS result detail of O 1 <i>s</i> of Au- δ	7
Table S3. The XPS result detail of Ce 3 <i>d</i> of Au- δ	8
Fig. S1. XPS spectra (Au 4 <i>f</i>) of: (a) Au-0.93, (b) Au-0.81, (c) Au-0.72, (d) Au-0.35, (e) Au-0.31, (f) Au-0.27.....	9
Fig. S2. XRD data of CeO ₂ and Au ₁ /CeO ₂ (100).	10
Fig. S3. (a) SEM and (b) HRTEM images of Au ₁ /CeO ₂ (100).....	11
Fig. S4. XRD data of CeO ₂ and Au-0.27. (b) HRTEM images of Au-0.27.	12
Fig. S5. XPS spectra (O 1 <i>s</i>) of: (a) Au-0.93, (b) Au-0.81, (c) Au-0.72, (d) Au-0.35, (e) Au-0.31, (f) Au-0.27.....	13
Fig. S6. XPS spectra (Ce 3 <i>d</i>) of: (a) Au-0.93, (b) Au-0.81, (c) Au-0.72, (d) Au-0.35, (e) Au-0.31, (f) Au-0.27.....	14
Fig. S7. Liner fitting result of TOF and the average valence state δ	15
Fig. S8. Arrhenius plots for R with E_a over Au- δ	16
Fig. S9. CO-DRIFT spectra of CeO ₂ , reduced CeO ₂ and Au-0.27.....	17
Fig. S10. CO-DRIFT spectra of (a) Au-0.93 and (b) Au-0.35 collected in the elevated temperature.....	18
Fig. S11. Reaction rates (R) as a function of (a) O ₂ partial pressure and (b) CO partial pressure in whole gas system system over Au-0.93 (black) and Au-0.35 (red) at 80 °C. Reaction orders were determined from the slope of each line.	19
Fig. S12. O ₂ -TPD result of Au-0.93 and Au-0.35.	20

Experimental Section

1.1. Catalyst Preparation.

CeO₂ nanocubes were prepared by using a reported hydrothermal method.¹ 0.868 g Ce(NO₃)₃·6H₂O was dissolved into 10 mL deionized water. An aqueous NaOH solution (C_{NaOH} = 6 M, 70 mL) was prepared and transferred into a 100 mL Teflon bottle. The Ce(NO₃)₃ solution was added into the Teflon bottle drop by drop and stirred for 30 minutes to form a lilac color milky slurry. The Teflon bottle was further sealed tightly in a stainless-steel autoclave and placed into a drying oven to proceed the hydrothermal treatment at 180 °C for 24 h. The white precipitates were washed with deionized water till the pH reached neutral and separated by using centrifuge. The pale-yellow powders of ceria nanocube support was obtained by drying the precipitates at 80 °C overnight and calcining in a muffle furnace at 400 °C for 4 h.

Au₁/CeO₂(100), with an Au loading of 0.11 wt. % with respect to CeO₂, was prepared by a reported deposition-precipitation method.² First of all, 1 g CeO₂ support was suspended in 50 mL deionized water and stirred on a magnetic stirrer for 15 min. 2.4 g ammonium carbonate was dissolved in 25 mL deionized water by stirring for 10 min. The solution was slowly added into the CeO₂ slurry. 5.7 mL of HAuCl₄ (2.3 mM) solution was added into the mixture drop by drop. Stirring was performed for 20 min at RT and the slurry was aged at room temperature for 1 h. The precipitates were washed with deionized water till the pH reached neutral and separated by using centrifuge. Au₁/CeO₂ powders were obtained after drying at 80 °C overnight.

1.2. Catalyst Characterization.

X-ray Diffraction (XRD) tests were performed on a D8 Advance X-ray diffractometer manufactured by Bruker, Germany. The X-ray light source was Cu K α radiation ($\lambda = 1.5406 \text{ \AA}$), Ni filtered, step size 0.02°. 2 theta (2θ) was in the range of 10-90°.

Scanning Electron Microscope (SEM) images were obtained on a SSX-550 instrument.

Transmission Electron Microscope (TEM and HRTEM) images were obtained on a Talos F200X G2 instrument.

Aberration-corrected high angle annular dark-field scanning transmission electron microscopy (AC-HAADF/STEM) images were obtained on a Fei-Titan Cubed Themis G2 300 instrument.

The XPS spectra of Au *4f*, O *1s*, and Ce *3d* were obtained by using an AXIS Ultra X-ray photoelectron spectrometer. To avoid the re-oxidation of the reduced samples in air before the ex-situ XPS test, we quickly transferred the reduced samples to a sealed tube and filled the tube with inert gas and sent the samples immediately. The samples treated with different reduction temperatures were also sent together in the same batch of preparation, which means that the conditions of the XPS test are identical, indicating that the difference of the XPS results between each sample can reflect the change of Au valence state. The specific fitting operation of Au *4f*, O *1s*, and Ce *3d* spectra was processed on XPSPEAK software. The binding energies were referenced using the maximum intensity of the advantageous C *1s* signal at 284.8 eV.

The actual loading of the synthesized sample was measured by inductive coupled plasma optical emission spectrometry (ICP-OES) conducted on a Thermo Scientific ICAP7600.

Temperature-programmed reduction by hydrogen (H_2 -TPR) was conducted on a TP-5080 adsorption instrument. 0.1 g catalyst was first pretreated at 200 °C in pure He (30 ml min⁻¹) for 1 h, with the ramping rate of 10 °C min⁻¹. After cooling down to room temperature, 5% H_2/Ar (50 ml min⁻¹) was used to reach a steady state. Then, the sample was heated from room temperature to 600 °C and the temperature was maintained at 600 °C for 30 min. The ramping rate was 10 °C min⁻¹. The outlet gas was detected by a TCD detector.

Temperature-programmed reduction by oxygen (O_2 -TPD) was performed on a Hiden Analytical QIC-20. 0.1 g catalyst was pretreated at 300 °C in pure He (30 ml min⁻¹) for 1 h with a ramping rate of 10 °C min⁻¹. After cooling down to room

temperature, O₂ (30 ml min⁻¹) was inlet for adsorption for 30 min, followed by purging with pure He (30 ml min⁻¹) for another hour. Then, the catalyst was heated from room temperature to 800 °C and the temperature was maintained at 800 °C for 30 min. The ramping rate was 10 °C min⁻¹. The outlet gas was detected by a TDC detector.

The in situ diffuse reflectance infrared Fourier transform spectra (DRIFTS) were recorded on a Nicolet iS 50 Fourier transform infrared (FTIR) spectrometer. The experiment was conducted under two different modes. For the adsorption-desorption mode, the sample was first pretreated at 300 °C in pure N₂ (100 ml min⁻¹) for 1 h. The background data was collected after pretreatment at 30 °C. After reaching room temperature, the gas flow was switched to 1% CO/He (50 ml min⁻¹) for 1 h. Then the catalyst was purged with pure He (50 ml min⁻¹) for 20 min to remove the physically adsorbed CO. The spectra were collected during the heating process by using the underground spectra before. For the steady-state mode, the sample was also pretreated in pure N₂ (100 ml min⁻¹) for 1 h. After cooling down to 30 °C, the adsorption of CO was conducted under 1% CO/He (50 ml min⁻¹) for 30 min. Pure He (50 ml min⁻¹) was introduced for 20 min and then the spectra were collected during the heating process with no gas flow.

1.3. Catalytic Evaluation.

The catalytic performances for CO oxidation were tested in the U-shaped quartz glass fixed-bed flow reactor at atmosphere pressure and the reactivity data was collected on a Gas chromatograph (Agilent, 7890B). The reaction conditions were set as followed: CO/O₂/N₂ = 1%/20%/79%, flow rate = 50 mL min⁻¹, catalyst 0.05 g, 40-60 mesh. The reaction temperature was increased from about -50 to 250 °C at a ramping rate of 2 °C min⁻¹. Before the CO oxidation reaction, the reduced samples were treated under 2 vol.% H₂ and 98 vol.% Ar (50 mL min⁻¹) from ambient temperature to the target temperature (100-300 °C) at a ramping rate of 2 °C min⁻¹ and stayed at the temperature for 2 h. The X_{CO} was calculated as:

$$X_{CO} = \frac{CO_{in} - CO_{out}}{CO_{in}} \times 100\%$$

where CO_{in} and CO_{out} denote the inlet concentration and outlet concentration of CO, respectively.

The TOF (CO converted numbers of single Au atom on CeO_2 catalyst per second) of CO oxidation was calculated as:

$$TOF = \frac{X_{CO} \times C_{CO} \times V_{CO} \times N_A}{\frac{V_m \times (T + 273.15)}{273.15} \times \frac{C_{Au} \times m_{cat} \times N_A}{M_{Au}}}$$

Where C_{CO} denotes the concentration in volume fraction of the fed CO, V_{CO} denotes the feed rate of CO ($L \text{ min}^{-1}$), N_A is the Avogadro constant, V_m is the standard molar volume of gas (22.4 L mol^{-1}), T is the reaction temperature when the conversion data was recorded, C_{Au} is the mass ratio of Au in Au/ CeO_2 catalyst, m_{cat} is the mass of catalysts and M_{Au} refers to the relative atomic mass of Au.

Tables and Figures

Table S1. The XPS result detail of Au- δ .

Catalysts	Au ⁰		Au ⁺		Au ³⁺		Average oxidation State (+ δ)
	<i>4f</i> _{5/2}	<i>4f</i> _{7/2}	<i>4f</i> _{5/2}	<i>4f</i> _{7/2}	<i>4f</i> _{5/2}	<i>4f</i> _{7/2}	
	87.33 eV	83.63 eV	88.07 eV	84.37 eV	89.23 eV	85.53 eV	
	FWHM (eV)	%	FWHM (eV)	%	FWHM (eV)	%	
Au-0.93	1.16	41.1	1.35	41.6	1.61	17.3	+0.93
Au-0.81	0.97	45.9	1.16	40.5	1.55	13.5	+0.81
Au-0.72	0.99	49.4	1.06	39.7	1.5	10.9	+0.72
Au-0.35	0.95	65.3	1.16	34.7	0	0	+0.35
Au-0.31	1.01	68.6	1.14	31.4	0	0	+0.31
Au-0.27	0.97	72.8	1.01	27.2	0	0	+0.27

*FWHM is the full width at half maxima of the XPS spectra.

Table S2. The XPS result detail of O 1s of Au- δ .

FWHM (eV) Peak (eV)		Catalysts					
		Au-0.93	Au-0.81	Au-0.72	Au-0.35	Au-0.31	Au-0.27
O_L	528.97	1.32	1.36	1.3	1.31	1.3	1.32
O_V	531.25	2.06	2.03	2.1	2.12	2.14	2.04
O_C	532.45	3	3.18	3.5	3.54	3.48	3.3

Table S3. The XPS result detail of Ce 3d of Au- δ .

FWHM (eV) Peak (eV)			Catalysts					
			Au-0.93	Au-0.81	Au-0.72	Au-0.35	Au-0.31	Au-0.27
Ce³⁺	u ⁰	902.4						
	v ⁰	883.9	3.26	3.36	3.45	3.36	3.34	3.69
	u [']	897.9						
	v [']	879.8	1.87	2.07	2.03	2.27	2.25	2.33
Ce⁴⁺	u	900.2						
	v	881.7	1.88	1.85	1.83	1.85	1.81	1.78
	u ^{''}	906.61						
	v ^{''}	888.0	3.26	3.36	3.45	3.36	3.34	3.69
	u ^{''} , ,	915.81						
	v ^{''} , ,	897.61	2.04	2.18	2.15	2.15	2.18	2.12

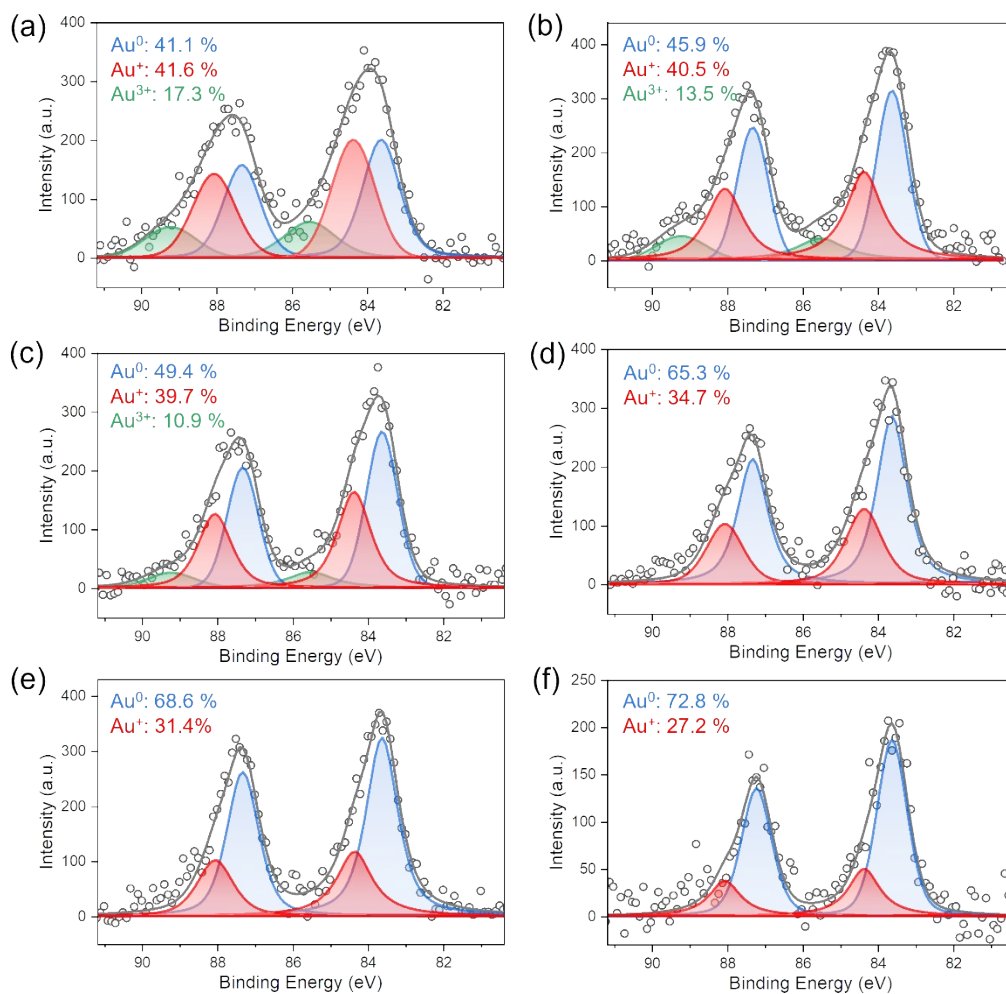


Fig. S1. XPS spectra (Au 4f) of: (a) Au-0.93, (b) Au-0.81, (c) Au-0.72, (d) Au-0.35, (e) Au-0.31, (f) Au-0.27.

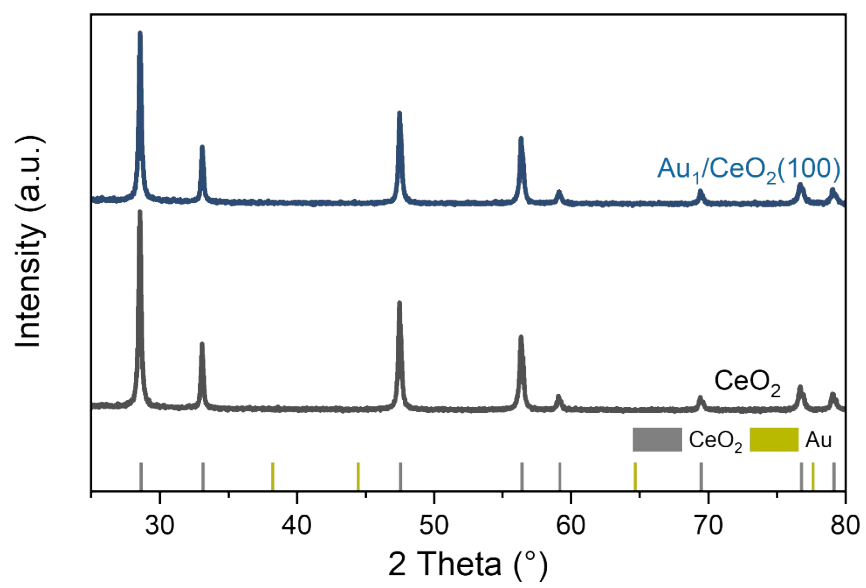


Fig. S2. XRD data of CeO₂ and Au₁/CeO₂(100).

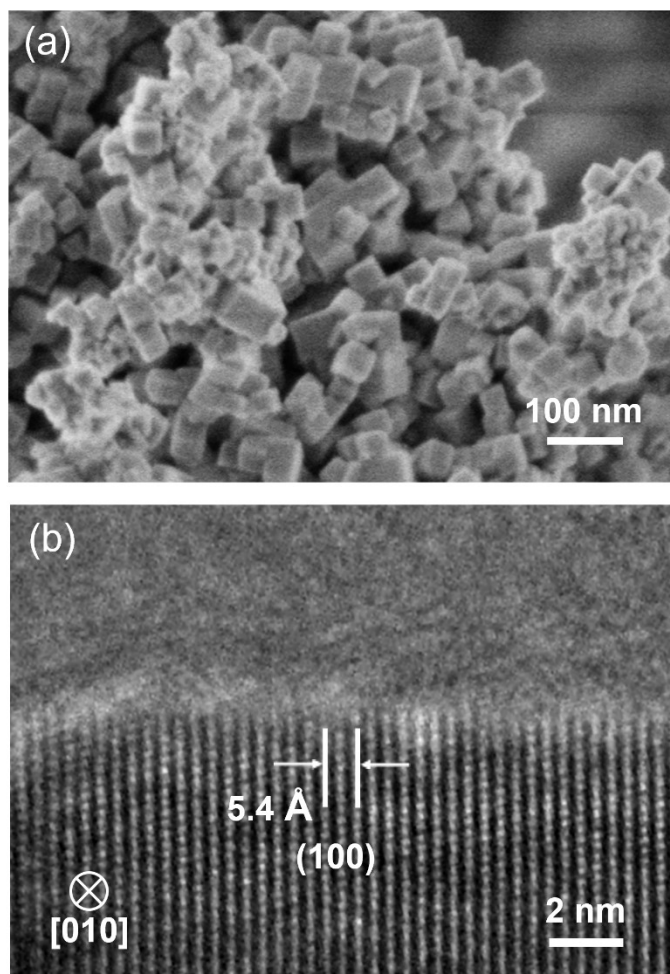


Fig. S3. (a) SEM and (b) HRTEM images of $\text{Au}_1/\text{CeO}_2(100)$.

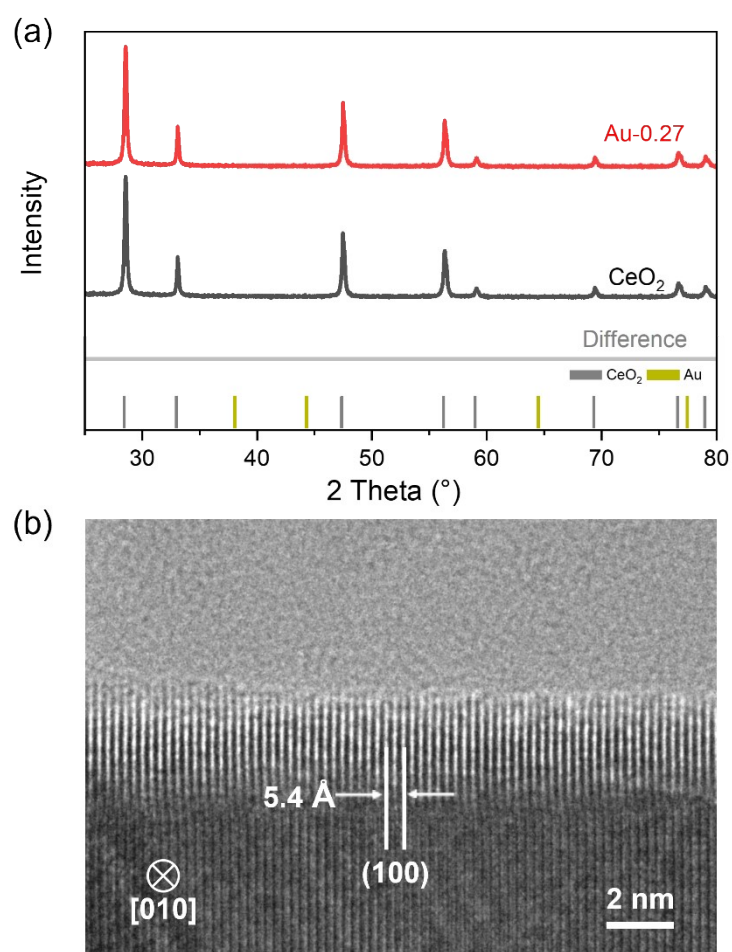


Fig. S4. (a) XRD data of CeO₂ and Au-0.27. (b) HRTEM image of Au-0.27.

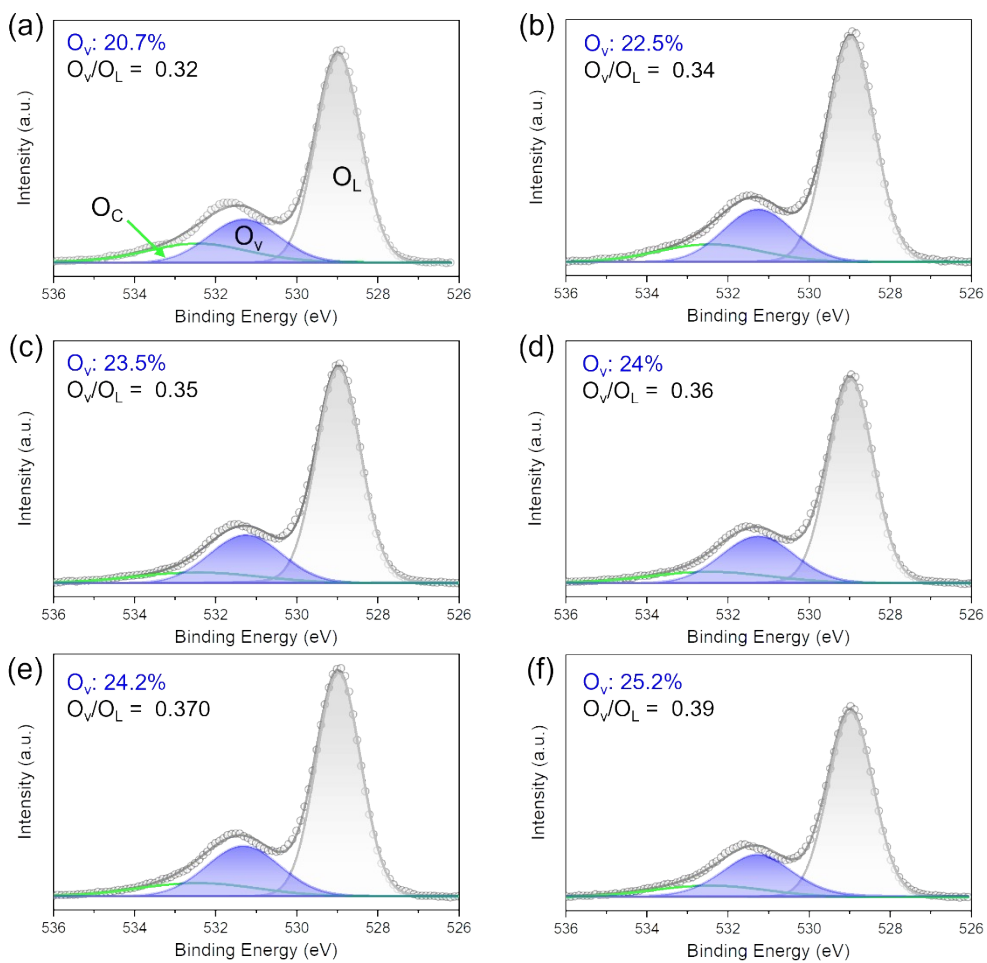


Fig. S5. XPS spectra (O 1s) of: (a) Au-0.93, (b) Au-0.81, (c) Au-0.72, (d) Au-0.35, (e) Au-0.31, (f) Au-0.27.

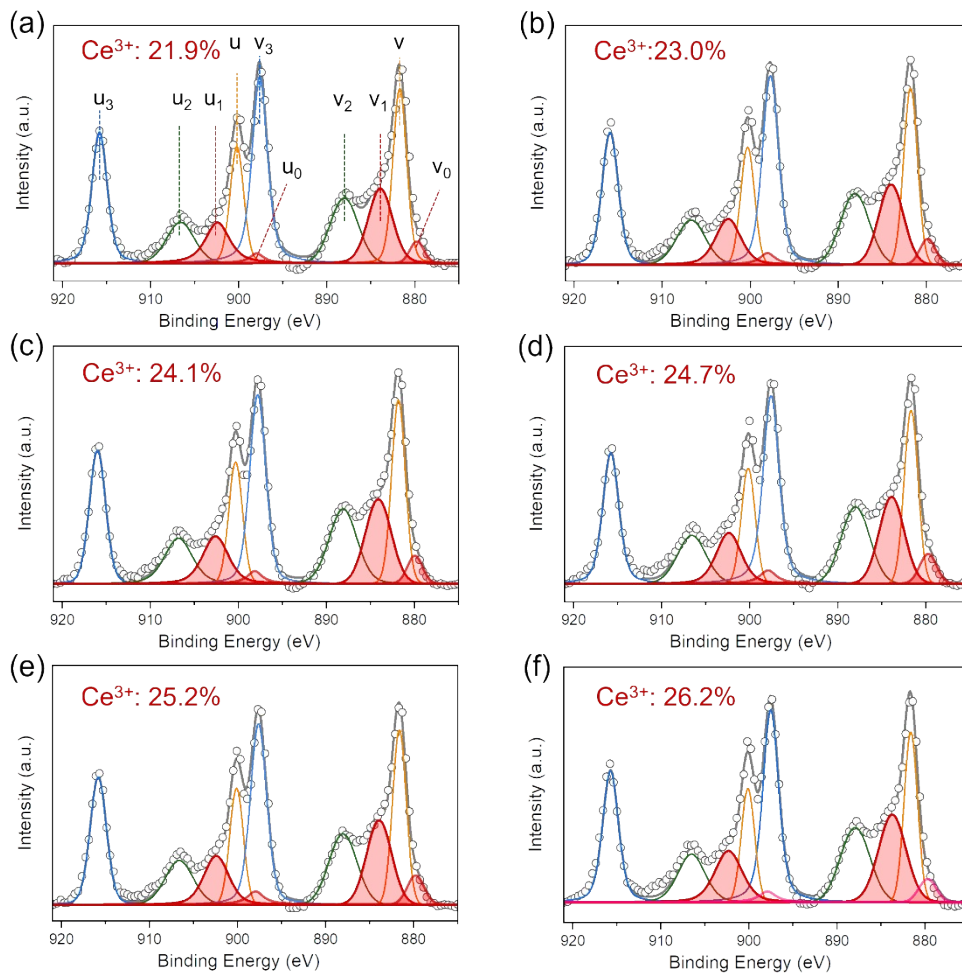


Fig. S6. XPS spectra (Ce 3d) of: (a) Au-0.93, (b) Au-0.81, (c) Au-0.72, (d) Au-0.35, (e) Au-0.31, (f) Au-0.27.

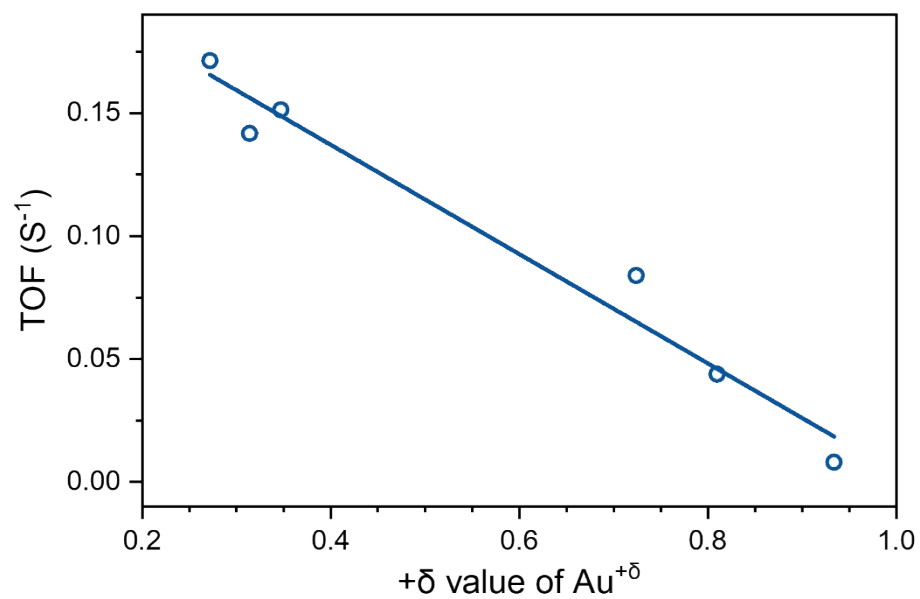


Fig. S7. Linear fitting result of TOF and the average valence state δ . The resulting equation is $y = -0.22x + 0.23, R^2 = 0.9664$.

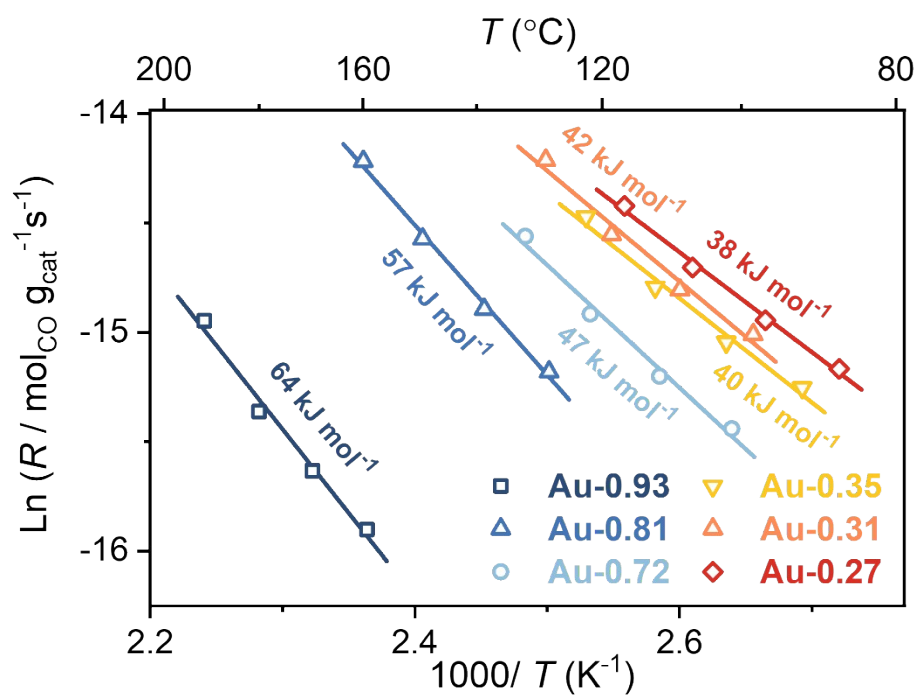


Fig. S8. Arrhenius plots for CO oxidation over Au- δ .

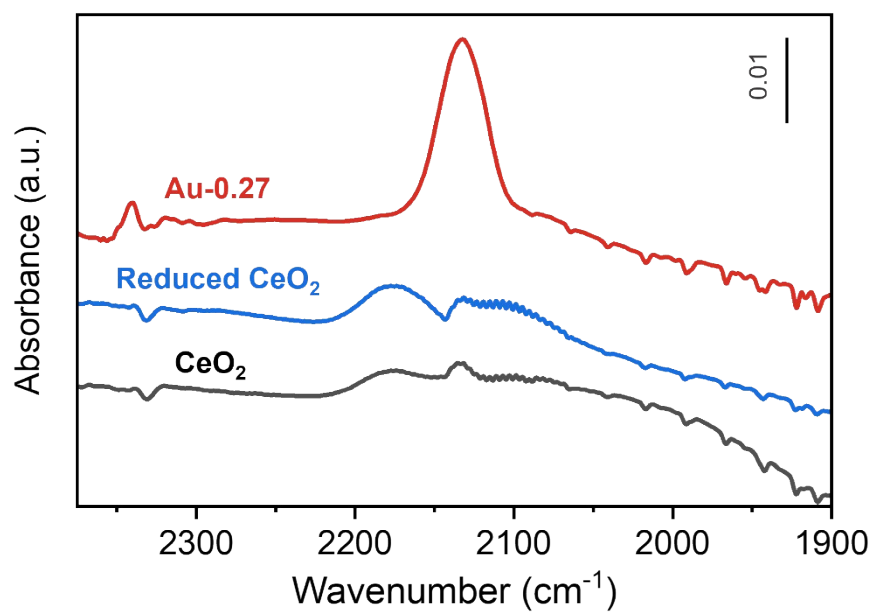


Fig. S9. CO-DRIFT spectra of CeO_2 , reduced CeO_2 and Au-0.27. The spectra of Au-0.27 was taken from Fig. 4 (a). The DRIFT spectra of CeO_2 and reduced CeO_2 were collected at room temperature after CO purging for 1 h and He purging for 10 min.

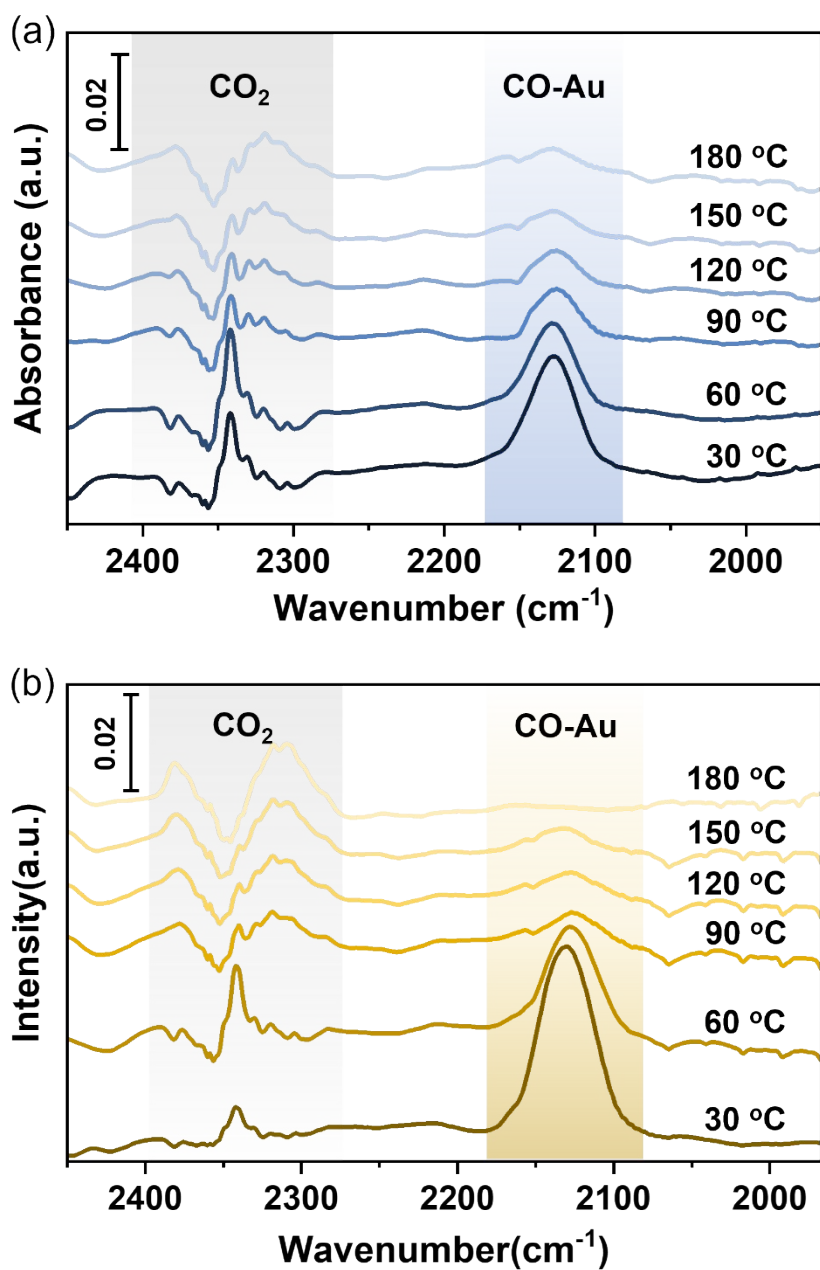


Fig. S10. CO-DRIFT spectra of (a) Au-0.93 and (b) Au-0.35 collected in the elevated temperature.

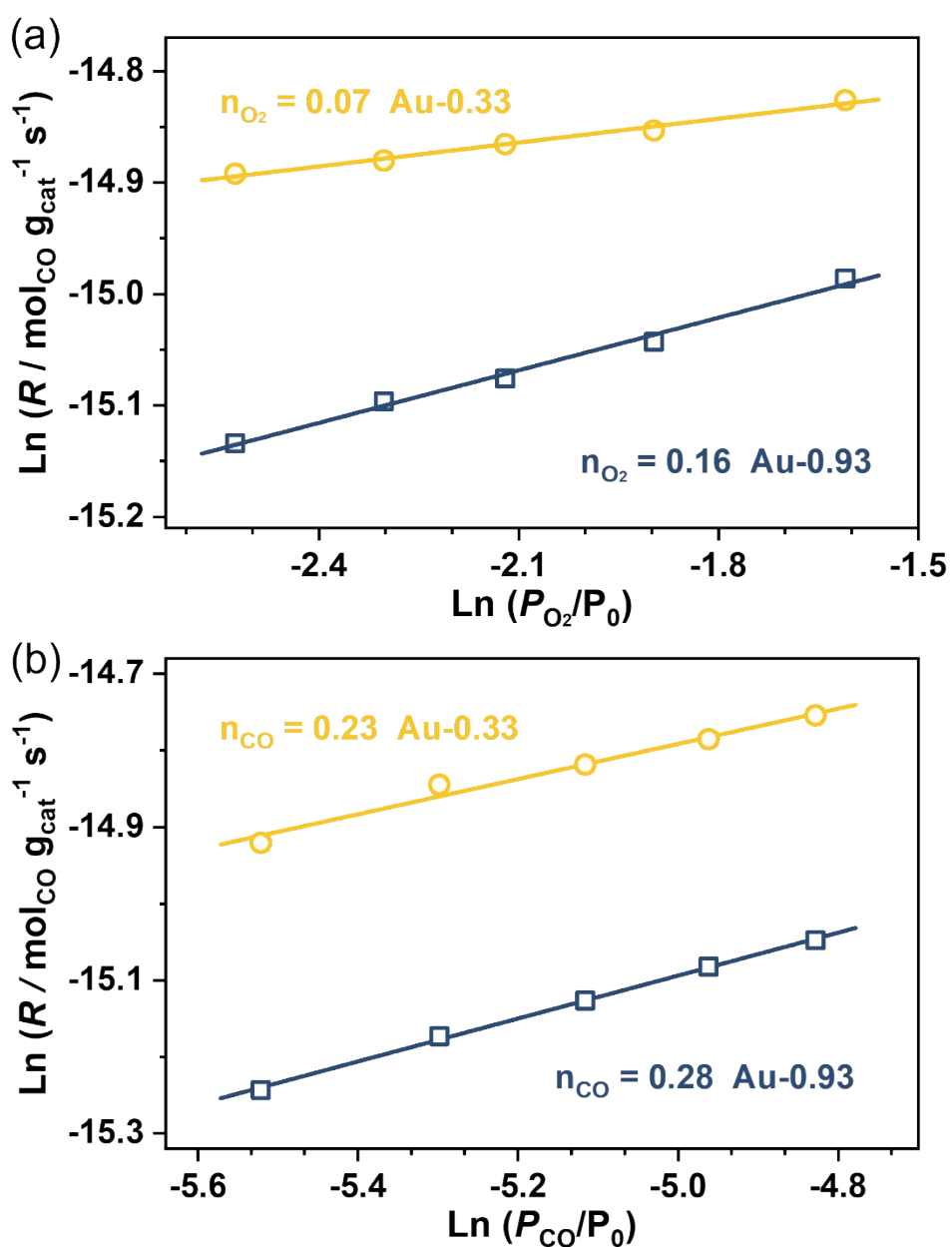


Fig. S11. Ln(R) (R, reaction rate) as a function of (a) O₂ partial pressure and (b) CO partial pressure in whole gas system system over Au-0.93 (yellow) and Au-0.35 (blue) at 80 °C. Reaction orders were determined from the slope of each line.

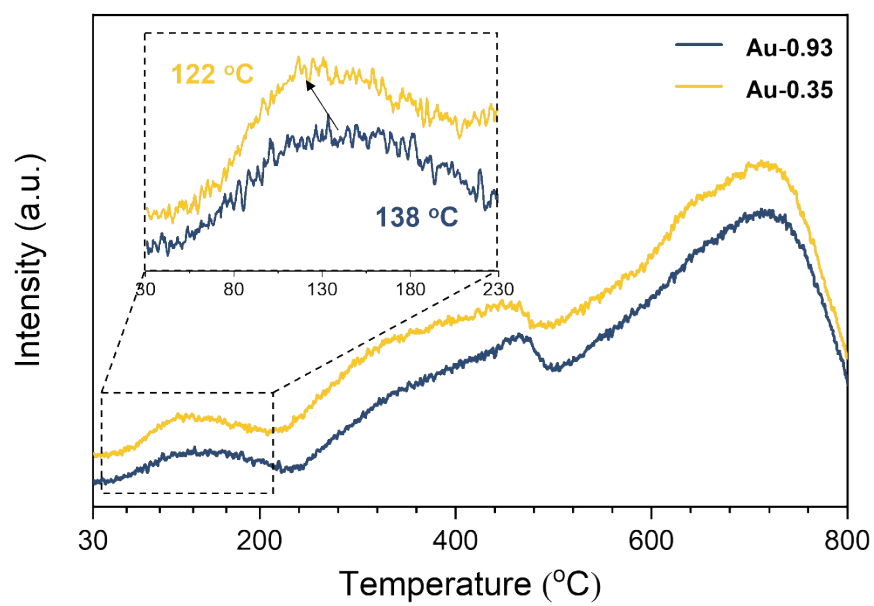


Fig. S12. O₂-TPD result of Au-0.93 and Au-0.35.

Reference

- 1 H.-X. Mai, L.-D. Sun, Y.-W. Zhang, R. Si, W. Feng, H.-P. Zhang, H.-C. Liu and C.-H. Yan, *J. Phys. Chem. B*, 2005, **109**, 24380.
- 2 L.-W. Guo, P.-P. Du, X.-P. Fu, C. Ma, J. Zeng, R. Si, Y.-Y. Huang, C.-J. Jia, Y.-W. Zhang and C.-H. Yan, *Nat. Commun.*, 2016, **7**, 1.